

Figure 2. MP2/6-31+G* neutral rotamers, n1–n9, of GABA optimized in the gas phase. For clarity, only terminal hydrogen atoms have been displayed. Intramolecular hydrogen bonds have been indicated as dotted lines.

In this paper we investigate the effectiveness of a number of possible solvation models in determining the structure and energetics of solution phase GABA. We set out to answer the specific questions:

1. What is the minimum level of theory that provides a realistic description of solvated GABA?
2. What are the role of short- and long-range solvent interactions in stabilizing GABA zwitterions?
3. What are the likely GABA structures in the aqueous phase?
4. Can approximate models be used to estimate the relative solvation free energies of GABA rotamers and tautomers?

II. Computational Methods

Stable rotamers of GABA have been optimized using Hartree–Fock (HF) theory, second-order many body Møller–Plesset Perturbation Theory (MP2)^{25–28} and density functional theory²⁹ utilizing the Becke-3–Lee–Yang–Parr (B3LYP) functional.³⁰ The 6-31+G* basis^{31–35} was used in all calculations. This is the smallest possible basis set required to span configuration space and account for hydrogen-bonding interactions and thus represents a tradeoff between computational expense and chemical accuracy.³⁶

In an attempt to isolate stable zwitterionic GABA rotamers, short-range solvent interactions were modeled by including explicit water molecules in the calculation as GABA monohydrate, GABA·H₂O, GABA dihydrate, GABA·2H₂O, and GABA pentahydrate, GABA·5H₂O. Mono- and dihydrated structures were optimized at B3LYP/6-31+G* and MP2/6-31+G*. Pentahydrated structures were optimized only at MP2/6-31+G*. GABA·H₂O did not form a stable zwitterion, and only the results for GABA·2H₂O and GABA·5H₂O are presented below.

The relative gas phase free energy of each optimized structure, $\Delta G(\text{gas})$, was determined at 310 K (37 °C) as the sum of the relative electronic energy, ΔE , the relative harmonic zero-point energy, ΔZPE , and the relative thermal free energy correction, $\Delta G_{\text{therm}} = \Delta H - T\Delta S$, calculated from the optimized geometry and harmonic frequencies of each species. These terms have

been included explicitly to indicate the relative values of the zero-point energy. A zero-point correction has not been included in ΔH .

Long-range solvent interactions for GABA, GABA·2H₂O, and GABA·5H₂O were modeled using the conductor-like screening solvation model (COSMO)^{37–39} with water ($\epsilon = 78.39$) as solvent. Stable neutral and zwitterionic rotamers of GABA were obtained by optimizing at B3LYP/6-31+G* in the COSMO reaction field. It was not possible to optimize MP2 wave functions in the reaction field. The effects of long-range solvent interactions were estimated for GABA·2H₂O using COSMO and the optimized gas phase structures of the dihydrate. Solvent effects were also estimated for the optimized dihydrate and pentahydrate structures by removing the explicit water molecules and placing the “dehydrated” GABA structures in the COSMO reaction field. Relative free energies of solvation at 310 K, ΔG_{solv} , were determined using COSMO for each optimized rotamer and relative solution phase free energies were calculated as $\Delta G(\text{solution}) = \Delta G(\text{gas}) + \Delta G_{\text{solv}}$. The structures and harmonic frequencies optimized at B3LYP/6-31+G* in the COSMO reaction field were used to provide an estimate of the solvation energy at MP2/6-31+G* for GABA.

All calculations reported here were carried out on the computing facilities in the School of Chemistry at the University of Sydney using Gaussian 98⁴⁰ and Turbomole 4.⁴¹

III. Results and Discussion

GABA. The lowest energy gas phase structure obtained for isolated GABA was neutral, independent of the level of theory used. No stable zwitterionic structures were found. As a consequence of its conformational flexibility, 9 neutral GABA rotamers, n1–n9, were identified. Each rotamer was optimized at each level of theory, and the B3LYP/6-31+G* optimized geometries are illustrated in Figure 2. Structures optimized at HF/6-31+G* and MP2/6-31+G* are similar to those shown in Figure 2. Rotamer n7 represents a fully extended structure, whereas rotamers n1, n3, n4, and n9 are “bent”, extended

TABLE 1: Characteristic Dihedral Angles (Figure 2), Relative Electronic Energy, ΔE , Harmonic Zero-Point Energy, ΔZPE , Thermal Free Energy, ΔG_{therm} , and Total Gas Phase Free Energy, $\Delta G(\text{gas})$, for Optimized Rotamers of GABA in the Gas Phase at the HF/6-31+G*, B3LYP/6-31+G*, and MP2/6-31+G* Levels of Theory^a

structure	HOOC-C-C-C dihedral angle	H ₂ N-C-C-C dihedral angle	ΔE	ΔZPE	ΔG_{therm}	$\Delta G(\text{gas})$
HF/6-31+G*						
n1	179.95	-61.38	3.9	0.9	-1.3	3.4
n2	94.05	-66.09	10.0	4.1	2.8	16.9
n3	173.56	63.07	7.3	0.2	-1.9	5.6
n4	63.31	178.19	6.3	0.0	-1.4	5.0
n5	56.94	56.55	4.1	1.3	-0.1	5.3
n6	-80.92	62.96	12.1	0.7	0.4	13.1
n7	178.81	-179.44	5.0	-0.3	-1.5	3.2
n8	-72.39	-61.81	0.0	0.0	0.0	0.0
n9	-73.27	179.68	2.5	-0.3	-0.3	1.9
B3LYP/6-31+G*						
n1	172.57	-62.67	0.0	0.0	0.0	0.0
n2	87.08	-67.97	-4.5	3.4	4.5	3.4
n3	-177.67	61.97	3.0	0.4	-0.9	2.5
n4	62.91	178.82	6.5	0.5	-0.9	6.0
n5	55.16	54.35	3.3	2.0	1.5	6.9
n6	-79.23	67.18	9.6	1.7	2.4	13.7
n7	176.72	177.53	3.1	-0.5	-1.0	1.6
n8	-60.65	-57.93	5.5	1.5	1.0	8.0
n9	-72.47	-179.89	2.8	0.3	0.5	3.7
MP2/6-31+G*						
n1	173.85	-62.05	0.0	0.0	0.0	0.0
n2	94.16	-65.67	-2.9	3.6	4.5	5.3
n3	-179.73	60.97	2.0	0.5	0.0	2.6
n4	58.57	178.50	4.6	0.8	0.5	5.8
n5	52.84	54.91	-1.9	2.3	2.7	3.0
n6	-79.48	61.26	5.7	1.5	3.1	10.3
n7	176.83	177.53	5.2	-0.4	-0.8	3.9
n8	-57.70	-56.98	0.1	2.0	2.9	5.0
n9	-69.81	179.12	2.3	0.4	0.8	3.6

^a All energies are in kJ/mol and are relative to the lowest free energy rotamer at each level of theory. Free energies are calculated at 310 K and $p = 1$ atm. $\Delta G_{\text{therm}} = \Delta H - T\Delta S$; $\Delta G(\text{gas}) = \Delta E + \Delta ZPE + \Delta G_{\text{therm}}$.

structures. Rotamers n5, n6, and n8 represent partially folded structures, and rotamer n2 is a folded, intramolecularly hydrogen-bonded structure. In general, rotation about the C-COOH bond resulted in identification of a second minimum energy structure of similar energy to the initial structure (within 2.5 kJ/mol), corresponding to moving the proton from its position on one oxygen atom to the other. The energy and conformation of only one of the conformers is reported here. The exception to this rule is the case of the intramolecularly hydrogen-bonded conformer, n2, where the carbonyl-bound proton is initially bound in an anti arrangement to the amine group. Rotation about the C-COOH bond yields no other stable rotamers, as the intramolecular hydrogen bond plays a significant role in the stabilization of this molecule. However, if the proton is moved to a syn configuration, an isomer of n6 is identified upon rotation about the C-COOH bond. The different rotamers can be characterized by the values of the HOOC-C-C-C and H₂N-C-C-C dihedral angles. The geometric and energetic results for each rotamer, at all levels of theory, are summarized in Table 1. The partially folded structure, n8, is lower in energy at HF/6-31+G*; however the extended structure, n1, is favored at B3LYP/6-31+G* and MP2/6-31+G*. The folded structures have higher harmonic zero-point energy at all levels of theory, although, even when zero-point and thermal free energy corrections are included to obtain a gas phase free energy at 310 K (37 °C) the folded structure remains most stable at HF/6-31+G*. The free energy differences at 310 K between structures n1 through n9 at HF/6-31+G* were relatively small: at most 17 kJ/mol. At B3LYP/6-31+G* and MP2/6-31+G*, all identified neutral rotamers had free energies within 14 kJ/mol. Given the relatively small basis set used, these free

energy differences are not significant and all nine neutral rotamers can be concluded to have similar stability.

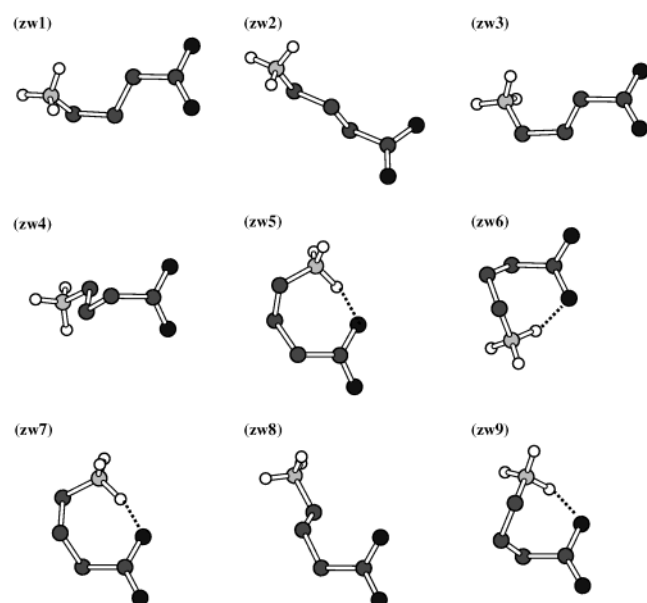
The results obtained using HF theory are qualitatively different from those obtained at B3LYP and MP2, indicating the importance of electron correlation in the description of molecules such as GABA. A similar conclusion has been reached in a previous study of glycine.¹⁴ The overall ordering of stability at B3LYP and MP2 is similar; the extended rotamers, in general, are more stable in the gas phase than the folded rotamers with rotamer n6 predicted to be the least stable by both methods.

Long-range solvent interactions with GABA were estimated using the COSMO polarized continuum model with a dielectric constant $\epsilon = 78.39$, corresponding to water. The solvation free energy was calculated using COSMO at geometries optimized in the reaction field at B3LYP/6-31+G*, and the results are summarized in Table 2. It is not possible to optimize structures in the COSMO reaction field at MP2. This procedure resulted in the identification of 18 optimized solvated structures: 9 neutral and 9 zwitterionic, corresponding to both extended and folded rotamers. These results differ from those of Odai et al.,²⁴ where only a single extended zwitterionic structure was optimized at HF/6-311G** in the COSMO reaction field. The 18 solvated neutral and zwitterionic rotamers we obtained are illustrated in Figure 3. It is apparent from Table 2 that the neutral rotamers, n1-n7 and n9, had similar electronic energies at B3LYP and that all the neutral structures were significantly more stable than any of the zwitterions. The neutral rotamers also had lower zero-point energies and thermal corrections than the zwitterions. Neutral molecules, however, do not significantly interact with an external electric field and the dielectric

TABLE 2: Characteristic Dihedral Angles (Figure 3), Relative Electronic Energy, ΔE , Harmonic Zero-Point Energy, ΔZPE , Thermal Free Energy, ΔG_{therm} , Solvation Free Energy, ΔG_{solv} , and Solution Phase Free Energy, $\Delta G(\text{solution})$ for Rotamers of GABA Optimized in the COSMO Reaction Field at the B3LYP/6-31+G* Level of Theory and Estimates of $\Delta G(\text{solution})$ at the MP2/6-31+G* Level of Theory^a

neutral	OOC–C–C–C dihedral angle	N–C–C–C dihedral angle	ΔE	ΔZPE	ΔG_{therm}	ΔG_{solv}	B3LYP/6-31+G* $\Delta G(\text{solution})$	MP2/6-31+G* $\Delta G(\text{solution})^b$
n1	177.58	−63.71	−75.6	−8.6	−3.8	120.1	32.0	35.7
n2	78.20	−70.30	−65.3	−6.8	0.5	94.0	22.4	29.9
n3	179.87	62.67	−69.4	−7.8	−4.3	115.4	33.9	39.1
n4	65.67	179.76	−69.6	−8.0	−0.4	117.2	39.3	41.0
n5	64.23	65.75	−70.4	−6.7	−3.3	120.8	40.4	40.5
n6	−74.42	68.52	−67.4	−6.4	−3.5	121.8	44.5	44.5
n7	178.75	179.81	−72.3	−8.3	−4.9	116.1	30.5	35.4
n8	−62.85	−64.83	−40.9	−6.6	−2.4	98.9	49.0	42.8
n9	−72.79	−177.41	−72.7	−7.7	−3.6	118.4	34.3	29.3
zwitterion								
zw1	−176.43	−67.02	160.5	−0.4	−3.7	−138.6	17.8	13.0
zw2	178.71	179.19	178.1	1.1	−1.9	−157.5	19.8	15.9
zw3	177.92	65.77	160.0	0.0	−3.7	−138.0	18.4	13.6
zw4	−63.06	−174.27	152.0	−0.6	−0.9	−130.8	19.7	13.2
zw5	−74.81	76.29	−0.1	−0.6	3.4	0.2	3.0	3.1
zw6	−45.26	−41.83	15.6	2.1	1.4	−6.3	12.9	7.8
zw7	75.31	−76.34	0.0	0.0	0.0	0.0	0.0	0.0
zw8	69.09	178.38	139.8	−0.2	−4.5	−120.3	14.8	9.5
zw9	45.92	41.47	15.9	1.9	1.4	−6.2	12.9	8.1

^a All energies are in kJ/mol and are relative to the energy of zw7. Free energies are calculated at 310 K and $p = 1$ atm. $\Delta G_{\text{therm}} = \Delta H - T\Delta S$; $\Delta G(\text{solution}) = \Delta E + \Delta ZPE + \Delta G_{\text{therm}} + \Delta G_{\text{solvation}}$. ^b MP2 calculations in the COSMO reaction field were performed using optimized B3LYP/6-31+G* geometries and free energies estimated from the B3LYP/6-31+G* harmonic frequencies.

**Figure 3.** B3LYP/6-31+G* zwitterionic, zw1–zw9, rotamers of GABA optimized in the COSMO reaction field. Neutral rotamers are similar to the gas phase structures depicted in Figure 2. For clarity, only terminal hydrogen atoms have been displayed. Intramolecular hydrogen bonds have been indicated as dotted lines.

continuum model had little effect on their relative energies. Conversely, the zwitterionic structures were significantly stabilized by the COSMO reaction field. Although the folded zwitterions, zw5 and zw7, had the lowest electronic energies, the extended zwitterions, zw1–zw4 and zw8, were preferentially stabilized by the long-range solvent interactions. The extended zwitterions have significantly larger dipoles than the folded zwitterions: at B3LYP/6-31+G* the magnitude of the dipole moment for zwitterions zw1, zw2, zw3, zw4, and zw8 is approximately 25 D, the folded zwitterions, zw5, zw6, zw7, and zw9 all have dipole moments with a magnitude of approximately 16.5 D. The larger solvation free energies calculated for the extended zwitterionic structures are consistent

with the enhancement of electrical asymmetry expected from a dielectric continuum solvation model.³⁸ Despite the enhanced stabilization of extended rotamers, the lowest free energy structures in solution at 310 K were found to be the folded zwitterions, zw7 and zw5. The overall free energy differences at B3LYP/6-31+G* between all of the zwitterionic rotamers (and neutral rotamer n2), however, were small, at most 22.4 kJ/mol. Recent work by Boese and Handy suggests that errors associated with the B3LYP prediction of energetic parameters in substituted hydrocarbons are approximately 12 kJ/mol, with the average error observed for anionic and cationic species approximately 36 kJ/mol.⁴² These calculations employed a larger basis set than the one used here and thus the intrinsic errors associated with the B3LYP/6-31+G* method may be greater 12 kJ/mol. Consequently, the rotamers zw1–zw9 and n2 can be seen as having similar stabilities in solution.

Single point MP2 energy calculations in the COSMO reaction field were performed at the B3LYP/6-31+G* + COSMO optimized geometries to provide an estimate of the MP2/6-31+G* correction to the electronic energy and to the solvation energy of the rotamers. The B3LYP/6-31+G* + COSMO optimized frequencies were used to estimate thermal and harmonic zero-point energy corrections. These results are included in Table 2 and suggest that the B3LYP method underestimates the stability of the zwitterionic relative to neutral rotamers with respect to MP2. Examination of the contributions to the MP2 correction indicated that the difference between the B3LYP and MP2 results arose because MP2 predicted the magnitude of the dipole moments of the zwitterionic rotamers to be approximately 0.5 D larger than B3LYP. As a consequence, the COSMO reaction field better stabilized the MP2 zwitterions. Similar results have also been observed for acetaldoxime⁴³ and ethylenimine,⁴⁴ where the dipole moment predicted at MP2 is larger than that predicted at B3LYP.

The folded zwitterionic rotamers, zw7 and zw5, remain the most stable solution phase structures at MP2, although all of the zwitterionic structures have relative free energies within 16 kJ/mol and all but zw2 and zw3 lie within 13 kJ/mol of the minimum free energy structure. Despite the differences observed

TABLE 3: Characteristic Dihedral Angles (Figure 6), Relative Electronic Energy, ΔE , Harmonic Zero-Point Energy, ΔZPE , Thermal Free Energy, ΔG_{therm} , Gas Phase Free Energy, $\Delta G(\text{gas})$, COSMO Solvation Free Energy, ΔG_{solv} , and Solution Phase Free Energy, $\Delta G(\text{solution})$ for Optimized Gas Phase Rotamers of GABA \cdot 2H₂O and GABA \cdot 5H₂O at B3LYP/6-31+G* and MP2/6-31+G*^a

	OO-C-C-C dihedral angle	N-C-C-C dihedral angle	ΔE	ΔZPE	ΔG_{therm}	$\Delta G(\text{gas})$	ΔG_{solv}	$\Delta G(\text{solution})$
GABA \cdot 2H ₂ O								
n1	162.86 (162.36)	-73.04 (-73.71)	16.1 (-16.1)	-1.7 (5.5)	-7.2 (-1.1)	7.3 (-11.7)	29.7 (21.9)	37.0 (10.2)
n2	88.24 (82.77)	-62.29 (-62.81)	-8.2 (-38.3)	-0.1 (6.7)	-1.8 (-4.8)	-10.1 (-26.9)	40.5 (32.0)	30.4 (5.1)
n3	-177.65 (-174.68)	61.37 (58.00)	24.1 (-2.9)	-4.1 (1.8)	-9.7 (-5.6)	10.3 (-6.7)	25.8 (16.5)	36.1 (9.9)
n4	60.54 (63.95)	178.01 (179.53)	30.8 (-0.7)	-4.9 (1.7)	-10.4 (-5.7)	15.4 (-4.8)	20.8 (14.4)	36.2 (9.6)
n5	67.12 (70.47)	72.76 (73.08)	22.0 (10.3)	-3.0 (3.8)	-7.8 (-2.5)	11.2 (-9.0)	27.3 (18.9)	38.5 (9.9)
n6	-73.04 (-73.67)	50.82 (51.05)	15.3 (-11.0)	-3.0 (3.0)	-3.9 (4.4)	8.4 (-3.5)	41.3 (33.1)	49.7 (29.5)
n7	174.87	-174.72	24.1	-4.3	-11.1	8.7	23.9	32.7
n8	-66.93 (-69.55)	-66.12 (-66.14)	49.3 (13.9)	-4.8 (2.3)	-9.8 (-3.2)	34.7 (12.9)	13.3 (6.4)	48.0 (19.3)
n9	-64.72 (-74.09)	-173.80 (-177.93)	25.1 (-7.3)	-4.3 (1.8)	-11.7 (-6.4)	9.1 (-12.0)	20.5 (12.8)	29.6 (0.9)
zw1	-170.01 (-170.47)	-52.68 (-51.40)	109.5 (77.4)	0.6 (5.2)	-1.4 (5.5)	108.6 (88.2)	-131.5 (-116.1)	-22.9 (-27.9)
zw2	139.79 (146.73)	-167.93 (166.48)	105.4 (78.6)	0.5 (1.0)	-1.2 (2.0)	104.7 (81.7)	-89.8 (-86.5)	14.9 (-4.8)
zw3	166.83 (167.63)	53.76 (51.96)	109.9 (78.1)	0.9 (5.7)	-1.1 (6.3)	109.7 (90.0)	-133.3 (-116.6)	-23.6 (-26.5)
zw4 ^b								
zw5	-58.06 (-68.73)	109.13 (62.40)	5.3 (-18.1)	-0.5 (1.7)	-1.0 (8.2)	3.9 (-8.1)	-1.8 (2.3)	2.0 (-5.8)
zw6	-37.87	-47.67	8.3	2.1	-0.1	10.4	-25.7	-15.4
zw7	81.65 (78.42)	-66.43 (-68.34)	0.0 (0.0)	0.0 (0.0)	0.0 (0.0)	0.0 (0.0)	0.0 (0.0)	0.0 (0.0)
zw8 ^b								
zw9	37.63	47.78	8.3	2.1	-0.1	10.3	-26.4	-16.1
GABA \cdot 5H ₂ O								
zw1	174.15	-55.16	45.5	1.8	4.6	51.9		
zw2	-175.72	178.08	69.0	-1.7	-5.6	61.7		
zw3	-160.65	70.57	42.5	2.4	4.5	49.4		
zw4	-55.55	148.04	-6.7	8.4	11.9	13.6		
zw5	-47.11	85.09	-17.2	3.6	3.7	-9.9		
zw6	-41.35	-48.59	2.6	4.3	8.4	15.3		
zw7	80.84	-71.72	0.0	0.0	0.0	0.0		
zw8	59.68	-89.89	-9.1	8.3	10.9	10.1		
zw9	39.19	48.04	-10.7	2.8	2.6	-5.4		

^a All energies are in kJ/mol and are relative to the energy of zw7. Free energies are calculated at 310 K and $p = 1$ atm. $\Delta G_{\text{therm}} = \Delta H - T\Delta S$; $\Delta G(\text{solution}) = \Delta E + \Delta ZPE + \Delta G_{\text{therm}} + \Delta G_{\text{solv}}$. GABA \cdot 2H₂O results were calculated at MP2/6-31+G*, and results at B3LYP/6-31+G* are given in brackets; structures n7, zw6, and zw9 were not stable at B3LYP/6-31+G*. GABA \cdot 5H₂O electronic and solvation energies were calculated at MP2/6-31+G*. ^b Does not exist as a dihydrated zwitterion at these levels of theory.

in Table 2, the MP2 and B3LYP relative energies are similar and show similar trends, suggesting that the B3LYP method may be a useful computational compromise in systems such as solvated GABA.

Formation of the folded zwitterionic structure, zw7, from the folded neutral structure, n2, involves proton transfer from the carboxylic oxygen to the amino nitrogen. This process was investigated by incrementally increasing the OH distance in the gas phase n2 rotamer, optimizing all other parameters, and calculating the solvation free energy correction to the structure in the COSMO reaction field. The free energy barrier for formation of the zwitterion from the neutral molecule via intramolecular proton transfer was found to be less than 8 kJ/mol, with a barrier less than 32 kJ/mol for the reverse reaction. The barrier to intramolecular proton transfer in glycine has been previously estimated to be approximately 9.2 kJ/mol¹⁴ with a barrier to intermolecular proton transfer (that is, proton transfer mediated by a water molecule) estimated to be approximately 9 kJ/mol.¹⁵

Optimizations in the COSMO reaction field, however, are limited, in terms of the methods available, cumbersome, and problematic. Their accuracy and utility is examined below by determining the relative contributions of short- and long-range solvent interactions.

Explicitly Hydrated GABA. Short-range solvent effects were included by considering mono-, di-, and pentahydrated GABA. Mono- and dihydrated structures were examined at the B3LYP/6-31+G* level of theory using Gaussian 98.⁴⁰ GABA \cdot 2H₂O

and GABA \cdot 5H₂O were examined at MP2/6-31+G* using Turbomole.⁴¹ One water molecule was found to be insufficient to stabilize the zwitterionic form of GABA. The presence of two or five water molecules, however, enabled stable zwitterionic structures to be obtained. GABA \cdot 5H₂O was the largest complex that could be feasibly investigated.

The optimized gas phase GABA \cdot 2H₂O and GABA \cdot 5H₂O structures and relative energies are summarized in Table 3 and have been identified in terms of their OOC-C-C-C and N-C-C-C dihedral angles. Optimized GABA \cdot 2H₂O and GABA \cdot 5H₂O structures are illustrated in Figures 4 and 5, respectively. These structures have been labeled similarly to the GABA structures obtained by optimization in the COSMO reaction field, Table 2 and Figures 2 and 3.

Optimizations of GABA \cdot 2H₂O at MP2/6-31+G* located 9 neutral and 7 zwitterionic structures in both extended and folded conformations. Eight neutral and 5 zwitterionic structures were also optimized at B3LYP/6-31+G*. The n7 neutral rotamer and the zw6 and zw9 zwitterions were not stable at the B3LYP/6-31+G* level of theory, the zw4 and zw8 zwitterions were not stable as dihydrates at either B3LYP or MP2. The neutral folded, intramolecularly hydrogen-bonded structure, n2, had the lowest electronic energy and gas phase free energy at 310 K at both B3LYP and MP2. At both B3LYP and MP2 the lowest energy gas phase zwitterions corresponded to the folded structures, zw5 and zw7. The gas phase GABA \cdot 2H₂O zwitterions, however, were significantly less stable than the n2-folded neutral structure at both B3LYP and MP2, indicating that long-range solvent

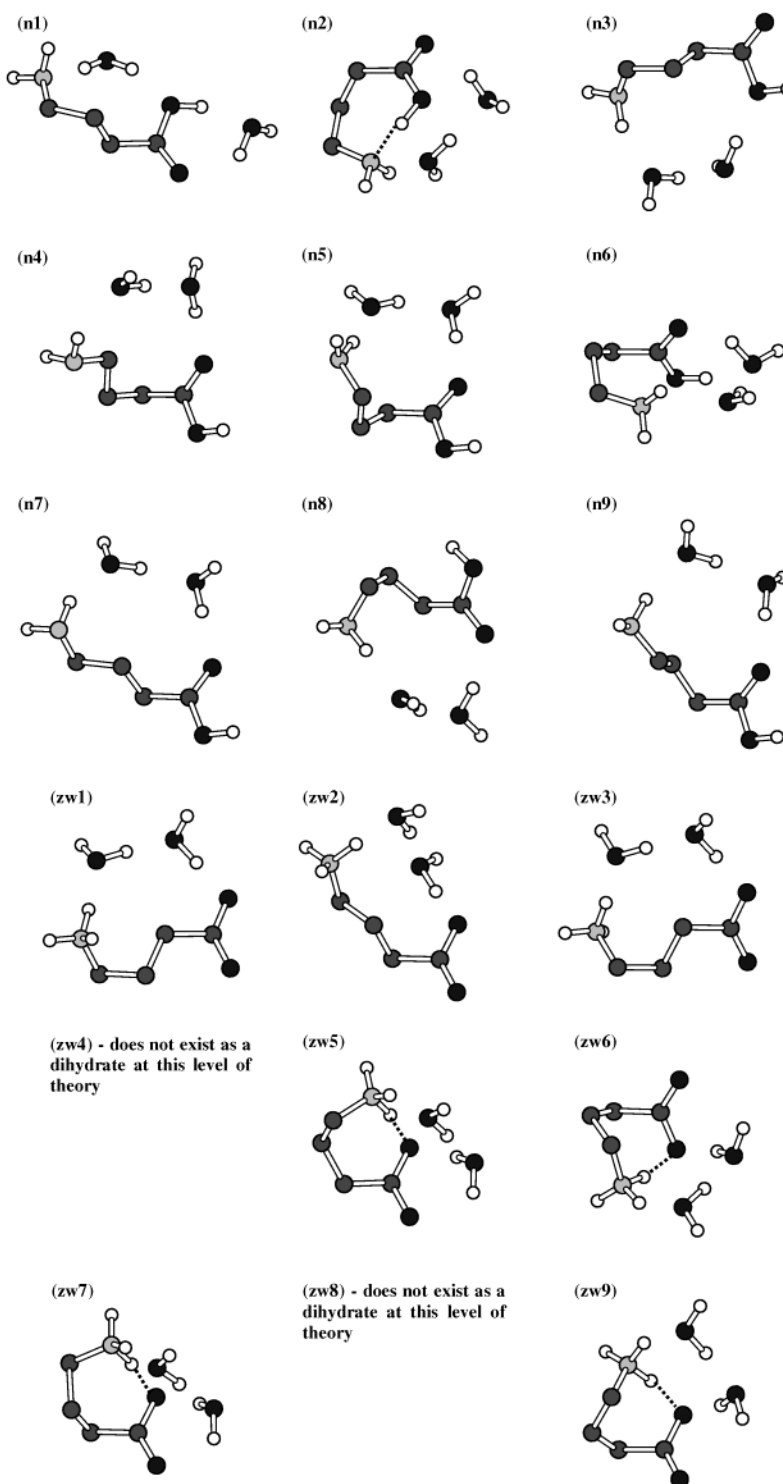


Figure 4. MP2/6-31+G* neutral and zwitterionic GABA·2H₂O optimized in the gas phase. For clarity, only terminal hydrogen atoms have been displayed. Intramolecular hydrogen bonds have been indicated as dotted lines.

interactions must play a significant role in the stabilization of the GABA zwitterion. The dihydrate approach alone is therefore insufficient to realistically determine the solution phase structure of GABA.

For the majority of zwitterionic GABA rotamers, a water molecule was found to be hydrogen bonded to both the carboxylate anion and the amino cation, with the two water molecules also hydrogen bonded to each other, forming a two-molecule bridge between the carboxylate and amino moieties. In the neutral GABA rotamers water molecules were typically hydrogen bonded to the amine and carboxylic acid groups, also

bridging the molecule. The exceptions were the neutral rotamer n1 and the folded zwitterionic rotamers zw5 and zw7. In these cases one water molecule was directly hydrogen bonded to one of the oxygen atoms of the carboxylate anion and the second water molecule formed a single-molecule bridge between the carboxylate anion and amino cation. We attempt to illustrate these complexes in Figure 4; however, full details of the geometries may be found in the Supporting Information.

The results obtained here for GABA·2H₂O differ from the HF/6-311++G** calculations of Ramek and Nagy.⁵ These calculations identified 5 neutral and 3 zwitterionic dihydrated

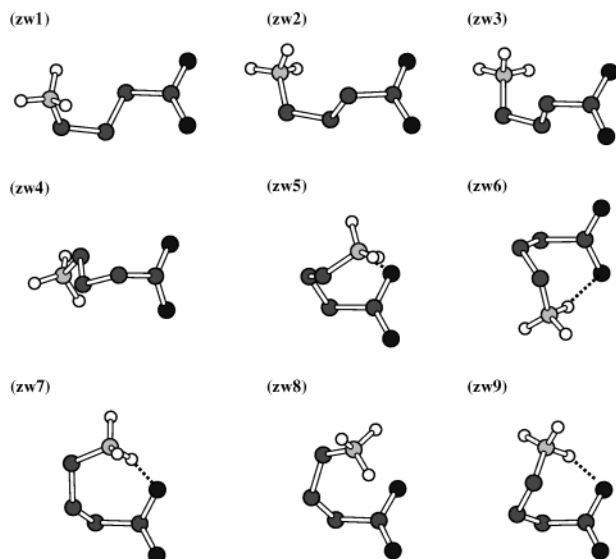


Figure 5. MP2/6-31+G* zwitterionic, zw1–zw9, rotamers of GABA·5H₂O optimized in the gas phase. The explicit water molecules have been removed for clarity, and only the terminal hydrogen atoms have been displayed. Intramolecular hydrogen bonds have been indicated as dotted lines.

structures with only one of the neutral structures and all 3 zwitterionic HF structures corresponding to structures identified in Table 3. In particular, Ramek and Nagy did not identify any extended neutral GABA·2H₂O structures and only a singly extended zwitterionic structure. The lowest energy structure they obtained corresponded to the n6 structure in Figure 4 and Table 3. These results, together with the calculations presented in Table 1, suggest that HF optimizations will not yield accurate structures for solvated GABA.

GABA·5H₂O was optimized at MP2/6-31+G* to 9 zwitterionic structures. No neutral structures were obtained, and it is clear that the presence of explicit binding to water plays an important role in stabilizing zwitterions. Both extended and folded zwitterions were observed, and the structures illustrated in Figure 5 are similar to those calculated when GABA was optimized in the COSMO reaction field (Figure 3), with the exception of zwitterions 4 and 8, which convert from more extended conformations to more folded conformations as a result of their interaction with the explicit water molecules. Although the water molecules have been omitted from Figure 5 for clarity, the 3-dimensional arrangement of the water around the GABA zwitterion generally involved two or more water molecules bridging between and hydrogen-bonded to the carboxylate and the amino moieties. Each complex generally possessed two such intermolecular bridges. The fifth water molecule was incorporated into this 3-dimensional arrangement either by binding exclusively to the carboxylate anion, by joining the bridging waters to create a bifurcated bridge, or by creating a three-membered bridge for more extended geometries. Although these configurations do not represent a comprehensive exploration of the conformational space, they do provide some examples of configurations that may be accessed in solution. The geometries of these complexes can be accessed in the included Supporting Information.

It is interesting to note that the positions of the water molecules around the GABA zwitterions change upon addition of an extra three water molecules relative to their positions in the conformers optimized with two waters. This suggests that, in solution, the water molecules are likely to move freely around the GABA zwitterion, although collectively retaining a role in

the stabilization of the molecule through bridging between the carboxylate and the amino groups.

The similarity of the structures obtained by optimizing GABA in COSMO and by optimizing GABA with explicit water molecules suggest that optimization of GABA in a continuum solvent can provide realistic starting geometries for more extensive optimizations involving explicit water molecules. The relative stabilities of the zwitterions obtained by optimizing GABA with COSMO, Table 2, and by optimizing GABA·5H₂O in the gas phase are also similar. The folded zwitterionic structures, zw5, zw7, and zw9, are the most stable GABA·5H₂O species, a result consistent with the gas phase stabilities of GABA·2H₂O. The fact that no neutral GABA·5H₂O structures were obtained suggests that solvated GABA is likely to exist only as a zwitterion.

Long-range solvent effects were estimated for GABA·2H₂O by application of the COSMO polarized continuum model. In general, optimization was not possible in the COSMO reaction field because of difficulties in forming fully enclosed, solvent accessible surfaces around the hydrated GABA structures. The solvation energy was therefore estimated by placing the optimized gas phase dihydrate structures in the reaction field. Relative solvation free energies and solution phase free energies for GABA·2H₂O are included in Table 3. It was not possible to obtain solution phase free energies for GABA·5H₂O. Similarly to the isolated GABA molecule and, as indicated in Table 3, the COSMO reaction field preferentially stabilized zwitterionic over neutral structures and preferentially stabilized extended over folded zwitterions. The dihydrated zw2 structure has a slightly smaller dipole moment, 14.7 D at MP2/6-31+G*, than the zw1 or zw3 structures, both approximately 16 D at MP2/6-31+G*, and was not as well stabilized by the solvent reaction field. At MP2/6-31+G* and B3LYP/6-31+G* the zwitterionic dihydrate structures all have lower solution phase free energies than the neutral rotamers. The lowest free energy GABA·2H₂O structures in solution correspond, in both cases, to the extended zwitterions, zw1 and zw3.

The most stable neutral rotamer in solution was the extended structure, n9. Solvation therefore also preferentially stabilizes extended neutral rotamers over folded rotamers. Given that intramolecular proton transfer is not possible in extended rotamers, these results suggest that the intermolecular proton transfer mechanism suggested by Jensen and Gordon¹⁵ may be responsible for zwitterion formation in solution.

Previous calculations have estimated the solvation energy of rotamers and tautomers of GABA·2H₂O⁵ and aspartic acid dihydrate²¹ by using the isolated molecular geometries optimized as hydrates. Given that optimization of GABA·2H₂O in the COSMO reaction field was problematic and that it was not possible even to estimate the solvation energy of GABA·5H₂O in the reaction field, the strengths and limitations of this approach have been investigated. Table 4 summarizes estimates of the MP2 solution phase free energy of the various GABA zwitterions: GABA·2H₂O optimized in the gas phase and placed in the COSMO reaction field, GABA optimized as GABA·2H₂O, then “dehydrated”, and placed in the COSMO reaction field, and GABA optimized as GABA·5H₂O, then “dehydrated”, and placed in the COSMO reaction field. As is apparent in Tables 2 and 3, application of the dielectric continuum solvent model had very little effect on the relative energy of the neutral rotamers, and these results have not been included. The results shown in Table 4 have been obtained using zero-point and thermal free energy corrections obtained from the harmonic frequencies of the optimized hydrated GABA structures such

TABLE 4: Relative MP2/6-31+G* Solution Phase Free Energies, $\Delta G(\text{solution})$, for GABA Zwitterions in the COSMO Reaction Field^a

species	dihydrate GABA·2H ₂ O	"dehydrate" GABA·2H ₂ O	"dehydrate" GABA·5H ₂ O
zw1	-22.9	-74.9	-84.9
zw2	14.9	-84.3	-88.5
zw3	-23.6	-75.2	-85.5
zw4			-79.7
zw5	2.0	2.4	-10.2
zw6	-15.4	-21.5	14.6
zw7	0.0	0.0	0.0
zw8			-31.7
zw9	-16.1	-21.3	-9.2

^a All energies are in kJ/mol and are relative to the energy of zw7. Free energies are calculated at 310 K and $p = 1$ atm. $\Delta G_{\text{therm}} = \Delta H - T\Delta S$; $\Delta G(\text{solution}) = \Delta E + \Delta \text{ZPE} + \Delta G_{\text{therm}} + \Delta G_{\text{solv}}$.

that $\Delta G(\text{solution})$ is the sum of $\Delta G(\text{gas})$ (from Table 3) and ΔG_{solv} , as calculated using COSMO. Comparison, in Table 4, of $\Delta G(\text{solution})$ of GABA·2H₂O and GABA, optimized as GABA·2H₂O and then "dehydrated", indicates that there are significant differences in the relative stabilities of the zwitterions. Removal of the two explicit water molecules significantly destabilized the zw1, zw2, zw5, zw6, zw7, and zw9 zwitterions with respect to the zw2 structure, incorrectly identifying zw2 as the most stable zwitterion in solution. All three extended zwitterions, zw1, zw2, and zw3, are significantly more stable using a "dehydrated" approach to the calculation of solvation free energy than when GABA·2H₂O is placed in the COSMO reaction field because the presence of the two explicit water molecules lowers the net dipole of the GABA·2H₂O complex, lowering ΔG_{solv} . This enhancement of the solvation free energy for the "dehydrated" extended structures is 99.2 kJ/mol for zw2 and approximately 52 kJ/mol for zw1 and zw3. Errors in the relative energies of the three extended zwitterionic structures are almost 50 kJ/mol. When "dehydrated" GABA·5H₂O was placed in the COSMO reaction field, the 4 extended zwitterions, zw1–zw4, were found to have similar stability and to be significantly more stable (by up to 93 kJ/mol) than the folded structures. Given the magnitude of the errors introduced in considering GABA·2H₂O, it is difficult to interpret these results. The results shown in Tables 2 and 3 do suggest, however, that extended structures are better stabilized by the COSMO reaction field. Given that the extended rotamers of GABA·5H₂O in the gas phase are relatively more stable than the extended rotamers of GABA·2H₂O in the gas phase, we suggest that solvation of the GABA zwitterion by successive addition of water molecules to the solvation sphere is likely to further stabilize extended structures relative to folded structures. Hence, extended rotamers are likely to dominate the aqueous phase structure of GABA. This is indeed consistent with experimental observation.^{8,9} Provided its limitations are identified, modeling solvation effects by placing "dehydrated" structures in a solvent reaction field (or indeed a Monte Carlo simulation) may be a useful computational compromise and may enable stable solution phase structures to be identified.

IV. Summary

The stabilization of GABA zwitterions in aqueous solution has been investigated at various levels of theory by considering both short- and long-range solvent interactions. Long-range interactions have been modeled using the conductor-like screening solvation model (COSMO) and short-range interactions have been examined by explicitly hydrating GABA with one, two or five water molecules.

A number of questions have been specifically addressed in this work and the answers are summarized below.

1. *What is the minimum level of theory that provides a realistic description of solvated GABA?* A comparison of the levels of theory used suggested that optimizations at the HF level of theory did not provide a realistic description of solvated GABA. Geometries, relative energies, and trends, however, were similar when computed at B3LYP or MP2. The B3LYP method may therefore be a practical compromise in systems such as solvated GABA with the caveat that zwitterions are better stabilized in solution at MP2 because of larger calculated dipoles. The determination of realistic solution phase structures for zwitterionic GABA was found to be dependent on the effective treatment of solvent–solute interactions. The only approaches that provided zwitterionic structures consistent with experiment were the application of a polarized continuum solvation model to GABA·2H₂O or GABA·5H₂O. A realistic description of aqueous phase GABA required both explicit interaction with at least two water molecules and long-range, dielectric interactions with the solvent.

2. *What are the roles of short- and long-range solvent interactions in stabilizing GABA zwitterions?* The inclusion of short-range solvent interactions via explicit water molecules preferentially stabilized zwitterionic over neutral structures. Long-range solvent interactions preferentially stabilized zwitterions over neutral tautomers and preferentially stabilized extended over folded rotamers in both neutral and zwitterionic species. Estimates of the solvation energies of the GABA·2H₂O and GABA·5H₂O rotamers further suggested that explicit water molecules bound to GABA preferentially stabilized the extended zwitterionic rotamers in solution.

3. *What are the likely GABA structures in the aqueous phase?* In the absence of any neutral GABA·5H₂O tautomers, neutral GABA is unlikely to exist in aqueous solution, and we conclude that only zwitterionic forms are present in water. The extended GABA·5H₂O zwitterions were postulated to be more stable in solution than the folded zwitterions, and it is likely that GABA exists in solution in a number of zwitterionic conformations.

4. *Can approximate models be used to estimate the relative solvation free energies of GABA rotamers and tautomers?* We have investigated the estimation of solvation energies by placing GABA, optimized as an explicit hydrate, in the COSMO reaction field. The free energies in solution of these "dehydrated" species differed by up to 99 kJ/mol from the explicitly hydrated GABA·2H₂O complexes. The relative stabilization of the extended rotamers was also significantly overestimated. This approach, however, may be the only feasible method for estimating long-range solvent interactions. It is therefore important to bear in mind the size and the nature of the errors introduced. It is also interesting to note that the optimization of isolated GABA in the COSMO reaction field yielded essentially the same 9 zwitterionic structures as obtained for GABA·5H₂O. Although the relative energies of these structures are not accurate in the absence of short-range solvent interactions, they provide a strategy for the identification and optimization of the explicitly hydrated system.

The results of this investigation suggest that zwitterionic forms of GABA are expected to exist in various, probably extended, conformations in aqueous solution at 310 K. It remains unclear, however, which conformation, or conformations, of GABA are biologically active.

Acknowledgment. D.L.C. acknowledges the financial support of an Australian Postgraduate Research Award.

Supporting Information Available: Geometries, energies, and harmonic frequencies of all structures described in this work may be obtained as Supporting Information. This material is available free of charge via the Internet at <http://pubs.acs.org>.

References and Notes

- (1) Rang, H. P.; Dale, M. M.; Ritter, J. M. In *Pharmacology*, 4th ed; Churchill Livingstone: Edinburgh, 1999; pp 478–480.
- (2) Prosser, H. M.; Dill, C. H.; Hirst, W. D.; Grau, E.; Robbins, M.; Calver, A.; Soffin, E. M.; Farmer, C. E.; Lanneau, C.; Gray, J.; Schenck, E.; Warmerdam, B. S.; Clapham, C.; Reavill, C.; Rogers, D. C.; Stean, T.; Upton, N.; Humphreys, K.; Randall, A.; Geppert, M.; Davies, C. H.; Pangalos, M. N. *Mol. Cell. Neurosci.* **2001**, *17*, 1059.
- (3) Bernard, C.; Cossart, R.; Hirsch, J. C.; Esclapez, M.; Ben-Ari, Y. *Epilepsia* **2000**, *41* (Suppl. 6), S90.
- (4) Leo, R. J. *Psychiatric Times* **2001**, XVII.
- (5) Ramek, M.; Nagy, P. I. *J. Phys. Chem. A* **2000**, *104*, 6844.
- (6) Weber, H.-P.; Craven, B. M.; McMullan, R. K. *Acta Crystallogr. B* **1983**, *39*, 360.
- (7) Tomita, K.; Higashi, H.; Fujiwara, T. *Bull. Chem. Soc. Jpn.* **1973**, *46*, 2199.
- (8) Tanaka, K.; Akutsu, H.; Ozaki, Y.; Kyogoku, Y.; Tomita, K.-I. *Bull. Chem. Soc. Jpn.* **1978**, *51*, 2654.
- (9) Ham, N. S. *Mol. Quantum Pharmacol., Proc 7th Jerusalem Symposium* **1974**, *7*, 261.
- (10) Ryan, J. A.; Whitten, J. J. *Am. Chem. Soc.* **1972**, *94*, 2396.
- (11) Tse, Y.-C.; Newton, M. D.; Vishveshwara, S.; Pople, J. A. *J. Am. Chem. Soc.* **1978**, *100*, 4329.
- (12) Ding, Y.; Krogh-Jespersen, K. *Chem. Phys. Lett.* **1972**, *199*, 261.
- (13) Tortonda, F. R.; Pascual-Ahuir, J. L.; Silla, E.; Tunon, I. *Chem. Phys. Lett.* **1996**, *260*, 21.
- (14) Kassab, E.; Langlet, J.; Evleth, E.; Akacem, Y. *J. Mol. Struct. (THEOCHEM)* **2000**, *531*, 267.
- (15) Jensen, J. H.; Gordon, M. S. *J. Am. Chem. Soc.* **1995**, *117*, 8157.
- (16) Ding, Y.; Krogh-Jespersen, K. *J. Comput. Chem.* **1996**, *17*, 338.
- (17) Kikuchi, O.; Matsuoda, T.; Sawahata, H.; Takahashi, O. *J. Mol. Struct. (THEOCHEM)* **1994**, *304*, 79.
- (18) Kinoshita, M.; Okamoto, Y.; Hirata, F. *J. Comput. Chem.* **1998**, *19*, 1724.
- (19) Ramirez, F. J.; Tunon, I.; Silla, E. *J. Phys. Chem. B* **1998**, *102*, 6290.
- (20) Smith, P. E.; Dang, L. X.; Pettitt, B. M. *J. Am. Chem. Soc.* **1991**, *113*, 67.
- (21) Nagy, P. I.; Noszal, B. *J. Phys. Chem. A* **2000**, *104*, 6834.
- (22) Lorenzini, M. L.; Bruno-Blanch, L.; Estiu, G. L. *J. Mol. Struct. (THEOCHEM)* **1998**, *454*, 1.
- (23) Lorenzini, M. L.; Bruno-Blanch, L.; Estiu, G. L. *Int. J. Quantum Chem.* **1998**, *70*, 1195.
- (24) Odai, K.; Sugimoto, T.; Kubo, M.; Ito, E. *J. Biochem. (Tokyo)* **2003**, *133*, 335.
- (25) Pople, J. A.; Binkley, J. S.; Seeger, R. *Int. J. Quantum Chem. Quantum Chem. Symp.* **1976**, *10*, 1.
- (26) Krishnan, R.; Pople, J. A. *Int. J. Quantum Chem.* **1978**, *14*, 91.
- (27) Bartlett, R. J.; Silver, D. M. *J. Chem. Phys.* **1975**, *62*, 3258.
- (28) Bartlett, R. J.; Purvis, G. D. *Int. J. Quantum Chem.* **1978**, *14*, 561.
- (29) Kohn, W.; Sham, L. J. *Phys. Rev. A* **1965**, *140*, 1133.
- (30) Becke, A. D. *J. Chem. Phys.* **1993**, *98*, 5648.
- (31) Ditchfield, R.; Hehre, W. J.; Pople, J. A. *J. Chem. Phys.* **1971**, *54*, 724.
- (32) Hehre, W. J.; Ditchfield, R.; Pople, J. A. *J. Chem. Phys.* **1972**, *56*, 2257.
- (33) Hariharan, P. C.; Pople, J. A. *Theo. Chim. Acta* **1973**, *28*, 213.
- (34) Clark, T.; Chandrasekhar, J.; Spitznagel, G. W.; Schleyer, P. v. R. *J. Comput. Chem.* **1982**, *3*, 363.
- (35) Clark, T.; Chandrasekhar, J.; Spitznagel, G. W.; Schleyer, P. v. R. *J. Comput. Chem.* **1983**, *4*, 294.
- (36) Levine, I. N. *Quantum Chemistry*, 5th ed.; Prentice Hall: New Jersey, 2000.
- (37) Klamt, A.; Schuurmann, G. *J. Chem. Soc., Perkin Trans. 2* **1993**, 799.
- (38) Klamt, A. In *Encyclopedia of Computational Chemistry*; Schleyer, P., Ed.; J. Wiley & Sons: Chichester, U.K., 1998; pp 604–615.
- (39) Barone, V.; Cossi, M.; Tomasi, J. *J. Comput. Chem.* **1998**, *19*, 404.
- (40) Frisch, M. J.; Trucks, G. W.; Schlegel, H. B.; Scuseria, G. E.; Robb, M. A.; Cheeseman, J. R.; Zakrzewski, V. G.; Montgomery, J. A., Jr.; Stratmann, R. E.; Burant, J. C.; Dapprich, S.; Millam, J. M.; Daniels, A. D.; Kudin, K. N.; Strain, M. C.; Farkas, O.; Tomasi, J.; Barone, V.; Cossi, M.; Cammi, R.; Mennucci, B.; Pomelli, C.; Adamo, C.; Clifford, S.; Ochterski, J.; Petersson, G. A.; Ayala, P. Y.; Cui, J.; Morokuma, K.; Malick, D. K.; Rabuck, A. D.; Raghavachari, K.; Foresman, J. B.; Cioslowski, J.; Ortiz, J. V.; Baboul, A. G.; Stefanov, B. B.; Liu, G.; Liashenko, A.; Piskorz, P.; Komaromi, I.; Gomperts, R.; Martin, R. L.; Fox, D. J.; Keith, T.; Al-Laham, M. A.; Peng, C. Y.; Nanayakkara, A.; Gonzalez, C.; Challacombe, M.; Gill, P. M. W.; Johnson, B.; Chen, W.; Wong, M. W.; Andres, J. L.; Gonzalez, C.; Head-Gordon, M.; Replogle, E. S.; Pople, J. A. *Gaussian 98*, Revision A.7; Gaussian, Inc.: Pittsburgh, PA, 1998.
- (41) Ahlrichs, R.; Bär, M.; Häser, M.; Horn, H.; Kölmel, C., *Chem. Phys. Lett.* **1989**, *162*, 165.
- (42) Boese, A. D.; Handy, N. C. *J. Chem. Phys.* **2001**, *114*, 5497.
- (43) Andrzejewska, A.; Lapinski, L.; Reva, I.; Fausto, R. *Phys. Chem. Chem. Phys.* **2002**, *4*, 3289.
- (44) Thorwirth, S.; Müller, H. S. P.; Winnemisser, G. *J. Mol. Spectrosc.* **2000**, *199*, 116.